PRODUCTION OF NEUTRON-DEFICIENT ASTATINE AND RADON ISOTOPES IN COMPLETE-FUSION REACTIONS*

A. Sitarčík

Department of Nuclear Physics and Biophysics
Comenius University in Bratislava
84248 Bratislava, Slovakia

Received 10 November 2023, accepted 11 January 2024, published online 24 April 2024

The systematics of fission-barrier scaling in the complete-fusion reactions leading to neutron-deficient astatine and radon compound nuclei is derived and discussed. The available cross-section data complemented by the newly-analysed unpublished experimental data were compared with the theoretical calculations by the statistical model code Hivap. The linear trend between barrier scaling and the mass number of compound nuclei was observed. The calculations for the most neutron-deficient nuclei required a significantly larger decrease in the fission-barrier height to reproduce the experimental data. A potential effect of quasi-fission causing this sudden trend change is outlined.

DOI:10.5506/APhysPolBSupp.17.3-A22

1. Introduction

The complete fusion reactions represent one of a few possibilities to produce short-lived neutron-deficient isotopes. The precise theoretical calculations of the expected yields of the reaction are especially critical for the search for new isotopes, where the number of produced nuclei may be low. The comparison of the experimental results with theoretical predictions therefore provides valuable information about the accuracy and reliability of the calculations.

During the fusion–evaporation reactions, the kinetic energy of the projectile is distributed across the projectile–target system and an excited compound nucleus (CN) is formed. Dominantly, an excited CN may split into lighter fragments (fusion–fission). In other cases, the excessive energy is released in the form of nucleons and/or γ quanta and an evaporation residue

* Presented at the XXXVII Mazurian Lakes Conference on Physics, Piaski, Poland, 3–9 September, 2023.

(ER) is created. Alternatively, a process of quasi-fission (QF) can be a dominant outcome of some reactions. Quasi-fission occurs shortly after a projectile and a target nucleus come into contact, splitting the system into lighter fragments before a CN is formed. The QF characteristics were mapped with respect to the mean fissility parameter $X_{\mathrm{mean}} = 0.75X_{\mathrm{eff}} + 0.25X_{\mathrm{CN}}$ [1]. The X_{eff} term is the fissility regarding the projectile, target, and compound nucleus, and X_{CN} is a standard fissility parameter. In the study, the QF was observed in reactions with $X_{\mathrm{mean}} \gtrsim 0.68$ [1]. For more details regarding the calculations of fissility parameters, see Appendix C in Ref. [1].

A statistical model code Hivap [2] is one of the available tools for the theoretical calculations of the ER production cross sections. The Hivap calculations reach a sufficient accuracy combined with a relative simplicity of the input parameters. One of the important input parameters is the fission barrier height calculated according to the rotating liquid drop model ($B_{\mathrm{f}}^{\mathrm{RLD}}$) [3]. The total barrier height (B_{f}) is calculated as

$$B_{\mathrm{f}} = \mathrm{BF} \times B_{\mathrm{f}}^{\mathrm{RLD}} + \Delta W_{\mathrm{gs}}\,, \tag{1}$$

where ΔW_{gs} is a correction to the fission barrier, usually taken as the ground-state shell correction and BF is the barrier scaling factor. In the cross-section studies of bismuth and polonium isotopes ($Z = 83, 84$), a linear dependence of BF with respect to the mass number of the studied CNs has been shown [4].

2. Hivap calculations and experimental data

Two parametrizations were used in the Hivap calculations to better account for the sub-barrier fusion. In the first parametrization, referred to as an inverted parabola approach, the fusion barrier is approximated by an inverted harmonic oscillator potential. The second approach is denoted as barrier fluctuations, where the fusion barrier height is 'smeared' by a standard deviation, enhancing the resulting cross sections for sub-barrier reactions. Both approaches give the same results above the fusion barrier. Below the barrier, the inverted parabola approach systematically underestimates the calculated cross sections, while the values obtained by barrier fluctuation approach are often overestimated.

In this work, the literature cross-section data from 21 complete fusion reactions leading to astatine and radon nuclei were complemented by the data from complete fusion reactions $^{52}\mathrm{Cr} + {}^{147,149,150}\mathrm{Sm} \rightarrow {}^{199,201,202}\mathrm{Rn}^{*}$ measured at the SHIP separator (GSI, Darmstadt) [5]. The experimental cross-section values were compared with the Hivap calculations and for each reaction, an ideal BF value of the Hivap calculations best reproducing the experimental data was determined.

All analysed reactions were measured at several beam energies, enabling a reliable determination of the excitation functions of the evaporation channels. In the analysed reactions, the ERs were velocity-separated by the SHIP and identified by the time-position correlation method [5]. The main contribution to the uncertainty of the extracted cross-section values is attributed to the transmission of the SHIP separator, for which the value of 40(10)% was used for all analysed reactions.

3. Results and discussion

An example of the experimental data and Hivap calculations is shown in Fig. 1. All reactions used for the deduction of the BF parameters are summarized in Table 1. In some reactions, the deduction of the BF parameter was not possible or not reliable enough. These reactions were usually measured at energies below the fusion barrier, where the Hivap calculations may not reproduce the experimental data well. The experimental excitation functions were satisfactorily reproduced by the Hivap calculations with the uncertainty of 0.02 of the BF parameter.

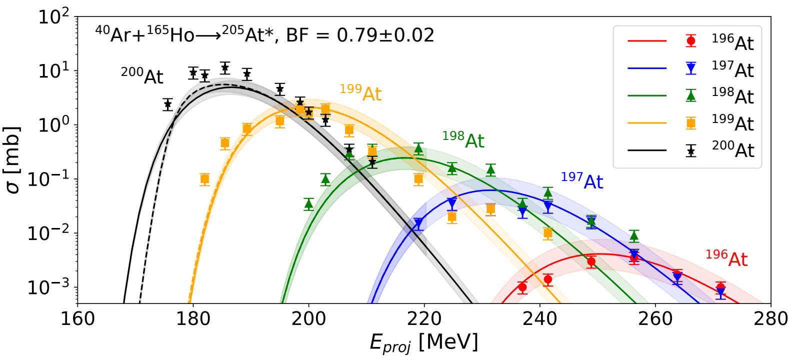

Fig. 1. An example of the experimental data (points) [6] and the theoretical excitation functions calculated by the statistical model code Hivap (lines) for the ^{40}Ar+^{165}Ho $\rightarrow$ ^{205}At* reaction. The solid lines denote the barrier fluctuations approach and the dashed lines denote the inverted parabola approach (see the text for details). Transparent shadows around the lines denote the Hivap calculations with BF$\pm$0.02.

The resulting systematics of BF scaling with respect to the mass number of the CNs is plotted in Fig. 2. Both radon and astatine CNs with $A \geq 195$ and 198, respectively, show a similar linear trend, however, with a slightly steeper slope than in the case of bismuth and polonium CNs (see Fig. 4 of [4] for comparison). Reactions leading to lighter compound nuclei (namely reactions number 2 and 16 from Table 1) display a change in the trend, requiring much lower BF values to ideally reproduce the experimental data.

Table 1. Reactions used in this work to deduce the barrier-scaling parameter. The uncertain BF values are denoted by *italics*. The reaction denoted by † was recently measured at the Argonne National Laboratory and the data are not published yet. The results from the reactions denoted by ‡ symbol are from unpublished data from the SHIP separator.

Reaction number	Reaction	CN	Ref.	X_{mean}	BF
1	^{93}Nb+^{99}Ru	^{192}At	†	0.757	
2	^{90}Zr+^{103}Rh	^{193}At	[7]	0.754	0.44
3	^{51}V+^{144}Sm	^{195}At	[8]	0.685	0.64
4	^{54}Fe+^{141}Pr	^{195}At	[9]	0.715	0.64
5	^{56}Fe+^{141}Pr	^{197}At	[10]	0.707	0.66
	^{56}Fe+^{141}Pr		[9, 11]		0.66
6	^{51}V+^{147}Sm	^{198}At	[12]	0.682	*0.67*
7	^{40}Ca+^{159}Tb	^{199}At	[13]	0.672	*0.76*
8	^{45}Sc+^{156}Gd	^{201}At	[14]	0.668	*0.65*
9	^{45}Sc+^{157}Gd	^{202}At	[14]	0.667	*0.70*
10	^{45}Sc+^{158}Gd	^{203}At	[14]	0.666	*0.71*
11	^{44}Ca+^{159}Tb	^{203}At	[15]	0.654	0.69
12	^{40}Ar+^{165}Ho	^{205}At	[16]	0.632	0.79
	^{40}Ar+^{165}Ho		[6]		0.79
	^{40}Ar+^{165}Ho		[17]		*0.74*
	^{40}Ar+^{165}Ho		[18]		0.79
13	^{24}Mg+^{181}Ta	^{205}At	[6]	0.574	0.78
14	^{26}Mg+^{181}Ta	^{207}At	[13]	0.561	0.81
15	^{48}Ca+^{159}Tb	^{207}At	[19]	0.638	0.82
16	^{52}Cr+^{144}Sm	^{196}Rn	[20]	0.704	0.51
17	^{56}Fe+^{142}Nd	^{198}Rn	[21]	0.715	0.62
18	^{52}Cr+^{147}Sm	^{199}Rn	‡	0.700	0.66
19	^{82}Kr+^{118}Sn	^{200}Rn	[22]	0.746	0.67
20	^{52}Cr+^{149}Sm	^{201}Rn	‡	0.697	0.68
21	^{52}Cr+^{150}Sm	^{202}Rn	‡	0.696	0.68
22	^{36}Ar+^{166}Er	^{202}Rn	[23]	0.658	*0.74*
23	^{28}Si+^{176}Hf	^{204}Rn	[24]	0.609	0.70
24	^{44}Ca+^{162}Dy	^{206}Rn	[25]	0.659	0.72
25	^{48}Ca+^{162}Dy	^{210}Rn	[26]	0.643	*0.74*

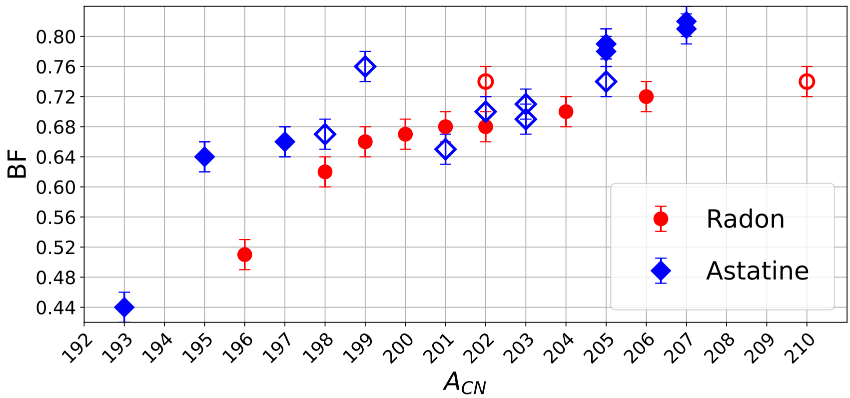

Fig. 2. (Colour on-line) Systematics of fission barrier scaling for radon (red dots) and astatine (blue diamonds) compound nuclei. The uncertain BF values are shown with empty symbols. These uncertainties are caused mainly due to sub-barrier reaction energies and difficulty to determine the ideal BF value. The uncertainties represent the BF value intervals (± 0.02), for which the experimental data were satisfactorily reproduced by the Hivap.

Such a change in the BF-scaling trend may be explained by an increasing influence of the quasi-fission hindering the creation of the compound nuclei. This assumption is also supported by the $X_{\rm mean}$ values of these reactions which are significantly higher than the $X_{\rm mean} = 0.68$ threshold observed in the QF study [1]. Results from a recently measured ^{93}Nb + ^{99}Ru $\rightarrow$ ^{192}At* reaction at the AGFA separator in Argonne National Laboratory (experiment number 2013 in [27]) may confirm this trend-breaking change and shed light onto an increasing effect of quasi-fission in the production of very neutron-deficient nuclei.

4. Conclusion

We derived the systematics of fission-barrier scaling in astatine and radon compound nuclei based on the comparison of the available experimental data and the theoretical Hivap calculations. The literature cross-section data were complemented by the data from four complete-fusion reactions measured at the SHIP separator. The linear dependence observed in the previous study of bismuth and polonium CNs was also observed in this study with a steeper trend and a sudden change in the slope in the most neutron-deficient isotopes. The potential influence of the quasi-fission on the production of very neutron-deficient isotopes was discussed.

This work was supported by the Slovak Research and Development Agency (contract number APVV-18-0268), by the Slovak grant agency VEGA (contract number 1/0651/21), and the Comenius University Youth Grant (contract number UK/286/2023). The new experimental data for ^{199,201,202}Rn* were provided by the SHIP Collaboration and the detailed analysis and results will be published elsewhere.

REFERENCES

[1] R. du Rietz *et al.*, *Phys. Rev. C* **88**, 054618 (2013).

[2] W. Reisdorf, *Z. Phys. A* **300**, 227 (1981).

[3] S. Cohen *et al.*, *Ann. Phys.* **82**, 557 (1974).

[4] A.N. Andreyev *et al.*, *Phys. Rev. C* **72**, 014612 (2005).

[5] G. Münzenberg *et al.*, *Nucl. Instrum. Methods* **161**, 65 (1979).

[6] A.N. Andreyev *et al.*, *Yad. Fiz.* **52**, (1990), https://www.osti.gov/etdeweb/biblio/5443016

[7] A.N. Andreyev *et al.*, *Phys. Rev. C* **108**, 034303 (2023).

[8] A.N. Andreyev *et al.*, *Phys. Rev. C* **73**, 024317 (2006).

[9] H. Kettunen *et al.*, *Eur. Phys. J. A* **17**, 537 (2003).

[10] B. Andel, «Study of Neutron-deficient Polonium Isotopes», Ph.D. Thesis, Comenius University in Bratislava, 2016.

[11] H. Kettunen *et al.*, *Eur. Phys. J. A* **16**, 457 (2003).

[12] M. Nyman *et al.*, *Phys. Rev. C* **88**, 054320 (2013).

[13] A.V. Yeremin *et al.*, *Phys. Atom. Nucl.* **66**, 1042 (2003).

[14] T.A. Werke *et al.*, *Phys. Rev. C* **92**, 034613 (2015).

[15] T.A. Werke *et al.*, *Phys. Rev. C* **92**, 054617 (2015).

[16] D. Vermeulen *et al.*, *Z. Phys. A* **318**, 157 (1984).

[17] U. Jakobsson *et al.*, *Phys. Rev. C* **82**, 044302 (2010).

[18] C.M. Folden III *et al.*, *Nucl. Instrum. Methods Phys. Res. A* **678**, 1 (2012).

[19] D.A. Mayorov *et al.*, *Phys. Rev. C* **90**, 024602 (2014).

[20] A.N. Andreyev *et al.*, *Phys. Rev. C* **74**, 064303 (2006).

[21] H. Kettunen *et al.*, *Phys. Rev. C* **63**, 044315 (2001).

[22] K. Andgren *et al.*, *Phys. Rev. C* **77**, 054303 (2008).

[23] R.B.E. Taylor *et al.*, *Phys. Rev. C* **59**, 673 (1999).

[24] R.B.E. Taylor *et al.*, *Phys. Rev. C* **54**, 2926 (1996).

[25] T.A. Werke *et al.*, *Phys. Rev. C* **92**, 054617 (2015).

[26] D.A. Mayorov *et al.*, *Phys. Rev. C* **92**, 054601 (2015).

[27] https://www.phy.anl.gov/atlas/pac/exp10May22.html